

# Accepted Manuscript

Mechanical properties and abrasive wear of white/brown coir epoxy composites

Petr Valášek, Roberto D'Amato, Miroslav Müller, Alessandro Ruggiero



PII: S1359-8368(18)30342-1

DOI: [10.1016/j.compositesb.2018.04.003](https://doi.org/10.1016/j.compositesb.2018.04.003)

Reference: JCOMB 5611

To appear in: *Composites Part B*

Received Date: 29 January 2018

Revised Date: 19 March 2018

Accepted Date: 3 April 2018

Please cite this article as: Valášek P, D'Amato R, Müller M, Ruggiero A, Mechanical properties and abrasive wear of white/brown coir epoxy composites, *Composites Part B* (2018), doi: 10.1016/j.compositesb.2018.04.003.

This is a PDF file of an unedited manuscript that has been accepted for publication. As a service to our customers we are providing this early version of the manuscript. The manuscript will undergo copyediting, typesetting, and review of the resulting proof before it is published in its final form. Please note that during the production process errors may be discovered which could affect the content, and all legal disclaimers that apply to the journal pertain.

# Mechanical properties and abrasive wear of white/brown coir epoxy composites

**Petr Valášek<sup>a</sup>, Roberto D'Amato<sup>b</sup>, Miroslav Müller<sup>a</sup>, Alessandro Ruggiero<sup>c</sup>,**

*<sup>a</sup>Czech University of Life Sciences Prague, Faculty of Engineering, Department of Material Science and Manufacturing Technology, Prague, Czech Republic*

*<sup>b</sup>Universidad Politécnica de Madrid, Departamento de Ingeniería Mecánica, Spain*

*<sup>c</sup>University of Salerno, Department of Industrial Engineering, Salerno, Italy*

## **Abstract.**

A substitution of synthetic fillers by natural fillers decreases an environmental burden, namely both in terms of saving fossil sources, and of a minimization of energy demands on a preparation of a reinforcement for composite systems. Last but not least the natural fibres are available and so they decrease a price of a final product. Performed experiment describes strength characteristics of white and brown coir fibres and biocomposites with the synthetic matrix and these fibres prepared by a vacuum infusion. Water solution of NaOH (6%, 12h) was used for treating of the fibre surface. The strength characteristics of the fibres differ depending on time of their harvesting – the tensile strength of previously harvested white fibres reached 115 MPa, the tensile strength of brown coir fibres harvested in a full maturity of the coconuts reached 123 MPa. The chemical treatment of the fibres led to roughening of the surface and to an improvement of an interfacial interaction. The chemical treatment of the fibres also led to the increase of their tensile strength up of 58 MPa (brown fibres) and the modulus was increased of 1.87 GPa on average. Globular formations on the surface of the fibres were removed due to the alkali acting. Layers of lignin were reduced which led to an improvement of the interaction with used epoxy resin. The inclusion of chemically treated brown fibres increased the matrix strength of 28.64 MPa, the inclusion of white fibres of 20.22 MPa.

**Key words:** Composites, Natural fillers, Mechanical properties, Abrasive wear.

## 1. Introduction

Composite materials with natural based phases are more desirable materials and vigorously developing area in a material engineering [1-4]. Biocomposites belong among very prospective composites which determine a direction of future materials, such as aerogel and other composites and materials [5-9]. Natural vegetable fibres have been already abundantly used in many industrial applications where just the vegetable fibres are of a dominant position comparing to the animal based fibres [10, 11]. Coir can be indicated as a renewable secondary natural resource. The strength of the natural fibres is determined above all by a content of cellulose [11]. A microfibrillar angle is proportional to a strain at break [11]. Coir belongs into a group of the cellulose based natural vegetable fibres [12, 13]. It is of many advantages. The strength, a high strain at break, a medical harmlessness and an availability influencing a low price of the fibres (the price ranges to 0,50 USD/kg) can be ranked among these advantages [13, 14]. A variability of characteristics owing to the biological essence of the material is the disadvantage. 0.45 mil tonnes of these fibres are produced annually according to Yan et al. [13, 14] in India and Sri Lanka above all. When comparing the coir with other types of the vegetable fibres it is possible to say that the coir is of lower cellulose content and higher microfibrillar angle. The utilization of the coir is possible in many applications, e.g. a production of composite boards, an application in the building industry – constructions of houses, parts of cars or also in a form of fillers into crash helmets [15].

The coir can be treated by alkali for increasing the strength characteristics of the composite system. This treatment leads to an improvement of surface properties in terms of a reduction of impurities and a lignin content. SEM analysis performed by the authors also proved better adhesion to matrices [16, 17]. Chemical treatments lead to the increase of the tensile strength and the impact strength of composite systems [18]. Easwara Prasad et al. [18]

optimized the impact strength of polymeric materials by the coir. The coir is also used for a creation of hybrid boards e.g. together with wood [19, 20].

Also coir dust is used in the interaction with epoxy matrices for increasing of the wear resistance.

The aims of the paper are following:

- an experimental description of strength characteristics of the coir harvested in various phases of a maturation of the coconut, i.e. the white and brown fibre,
- a description of the morphology of these fibres by means of an electron microscopy,
- a description of the pore structure in terms of the diameter size and porosity using mercury intrusion porosimetry technique [21, 22],
- a description of the influence of the fibre chemical treatment by the solution of NaOH on a change of the fibre surface structure,
- an experimental description of long-fibre composites with these fibres,
- an evaluation of the influence of the chemical treatment and a type of the fibre on the interfacial interaction with the reactoplastics synthetic matrix.

For this purpose, the abrasive wear under conditions of a no-rigidly (three-body abrasion resistance using sand feed into a contact zone between the specimen of the long-fibre composite and a rubber disc) was evaluated [23].

## **2. Material and methods**

In this section the type of used fibres and a resin will be presented. Furthermore, the methods used for the characterization of the treated fibres and the prepared composite will be described.

### ***2.1. Fibres***

The coir is reached from the fruits of the palm *Cocos nucifera* and it is a secondary product at processing of the fruits – coconuts (see Fig. 1).



**Fig. 1** Brown and white coir: fibres removed from coconut (left), fibres prepared for experimental program (right)

The coir is the most often gained mechanically in a line processing the coconuts when the fibres are removed from the coconuts (pectin packaging) by means of a set of counter-rotating rollers. The mechanization of this process minimizes or entirely removes the time needed for watering of coconuts before the fibres removing. The coir fibres gained from the technological line in Philippines were used in the experiment (Philippines belong among significant producers of coconuts). 100 g of fibres on average can be reached in the technological line from one mature coconut. The time of a maturation corresponds approx. to 40 - 50 days (according to the size of coconuts). The length of fibres ranges the most often in the interval 25 to 35 cm. Brown fibres which are the most often arising commodity are separated from matured coconuts. These fibres are used more than the white fibres. They are thicker and of wide applications. White fibres are extracted from immature coconuts, usually after 10 months of watering. White fibres are used e.g. for a production of ropes and nets resistant to salty water. Resultant fibre properties are given except for the biological character itself also by a method of the extraction itself and by the time before watering and extracting. The mechanical removing of fibres minimizes the influence of the watering – time reduction.

Defoirdt et al. [11] judged the density of the white coir  $1.01 \pm 0.05 \text{ g}\cdot\text{cm}^{-3}$  and of the brown coir  $1.29 \pm 0.07 \text{ g}\cdot\text{cm}^{-3}$ . Coconut fibre is of a natural microstructure (see Fig. 2). Its description is important for understanding the fibres behaviour and their interaction with the composite matrices.

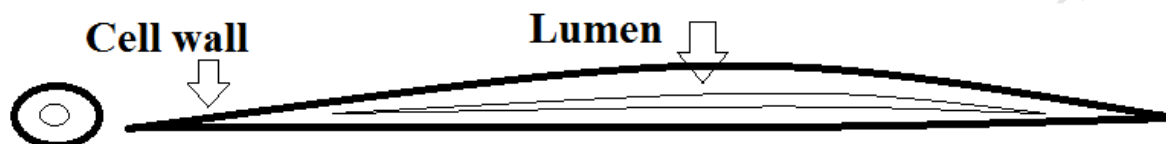


**Fig. 2** Structure of coir

The fibre surface treatment belongs among basic factors determining the interfacial interaction. It is important to summarize a chemical composition of the coir fibres in terms of this treatment, see Tab. 1.

6 % water solution of NaOH was used for the chemical treatment of the fibres, the time of acting 6 h at the laboratory temperature  $24 \pm 2 \text{ }^\circ\text{C}$ . Then all fibres were washed in a distilled water (including fibres without the chemical treatment) and dried at the temperature  $105 \text{ }^\circ\text{C}$ . The surface morphology not only in composite systems is one of the important aspects of engineering materials and their structures [24-27].

**Tab. 1** Chemical composition of coconut fibre (coir) [17, 20]

Cellulose (%)	Hemicellulose (%)	Pectin (%)	Lignin (%)	Density ( $\text{g}\cdot\text{cm}^{-3}$ )
46	0.3	4	45	1.15-1.46

A universal testing machine was used for the determination of the tensile characteristics of the fibres – it was used a modification of the standard ASTM C1557 (a length of fibres 10 mm, a shift speed corresponded to  $1 \text{ mm}\cdot\text{min}^{-1}$ ).

### 2.1.1. Porosimetry

The mercury porosimetry is the progressive intrusion of mercury, as adsorbate, into a pore structure under stringently controlled pressures. Mercury is forced into the pores of the solid by applying pressure. The value of the adsorbed mercury volume allows to calculate an area, a distribution by pore sizes, and percentage of porosity of the material. With this

technique pores between about mesopores (2-50 nm) and macropores (> 50 nm) can be investigated. The pore size distribution, the total pore volume or porosity, the skeletal and apparent density, and the specific surface area of a sample are the results of this characterization technique. It measures the largest entrance towards a pore (see Fig. 3), but not the real inner size of a pore. Furthermore, it cannot be used to analyse closed pores because the mercury has no way of entering in these pores. The non-wetting property and high surface tension of the mercury are the qualities for its use in the pore probing test.

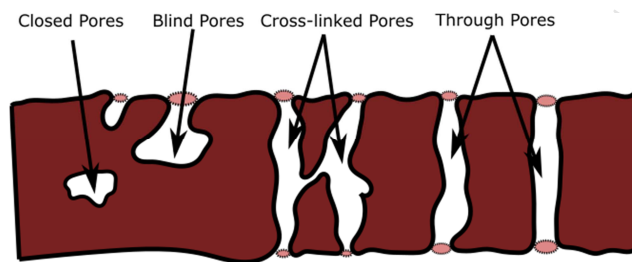


**Fig. 3** Schematic representation of pores

Mercury does not wet most substances and will not spontaneously penetrate pores by a capillary action, whereby it must be forced into the pores by the application of an external pressure. The required pressure is inversely proportional to the size of the pores. In fact, only slight pressure is required to force the mercury into large macropores, whereas for small pores much greater pressure is required. Clearly, more accurate pressure measurements result in more accurate pore size data. All porosimetry instruments adopt the assumption that the pore shapes are characterized as a cylindrical geometry. From the pressure versus intrusion data, the instrument used for this technique generates volume and size distributions by the Washburn [28] equation. The Equation (1) represents the balance between the force required to introduce the mercury in the pores and the force due to externally applied pressure acting over the area of the contact circle.

$$-\pi D\gamma \cos \theta = \frac{\pi D^2 P}{4} \quad (1)$$

or simplified

$$D_{pore} = \frac{-4\gamma \cos \theta}{P} \quad (2)$$

where  $D$  is the pore diameter,  $\gamma$  the surface tension,  $\theta$  the contact angle and  $P$  the applied pressure. The negative sign in equation (1) is because of  $\theta > 90^\circ$ . The first term is intrinsically negative (see Fig. 4).

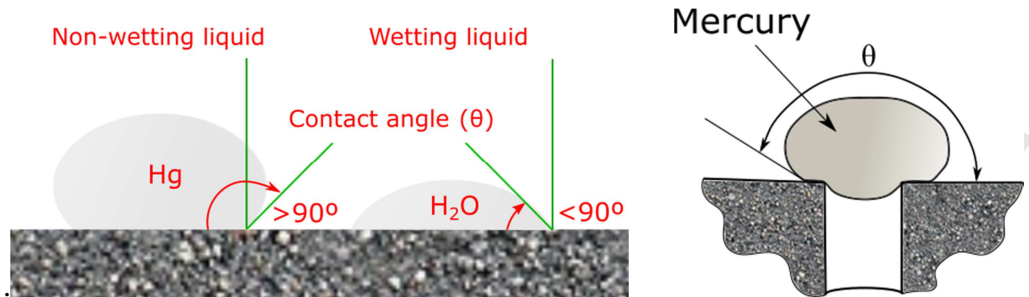


**Fig. 4** Liquids resting on solid surface. Different angles of contact are illustrated for wetting and non-wetting liquids (left); mercury in contact with porous solid (right).

The contact angle is a parameter which affects the analysis results. Numerous papers have demonstrated the wide range of the contact angles between mercury and various different or even very similar solid surfaces. For example, contact angles for "identical" systems of mercury on glass are of  $128^\circ$  to  $148^\circ$  [29]. On the other hand, a fixed value irrespective of the specific sample material is often applied in most practical situations, e.g.  $130^\circ$  or  $140^\circ$ . Several techniques are available to determine the contact angle. The contact angle can be also estimated using (3):

$$\cos \theta = 1 - \frac{\rho g h_{max}^2}{2\gamma_{Hg,air}} \quad (3)$$

where  $g$  is gravity acceleration, and  $\rho$  is density of the liquid.

In the case of materials composed of stacked, thin sheets where slit-like openings predominate, the expression of equation (2) will be:

$$W = \frac{-2\gamma \cos \theta}{P} \quad (4)$$

where  $W$  is the width between the pores. As above mentioned, the volume of mercury forced into pores (and into void spaces) increases as the pressure increases and as a result it is possible to obtain a unique pressure-volume curve. A few examples are shown in Fig. 5.



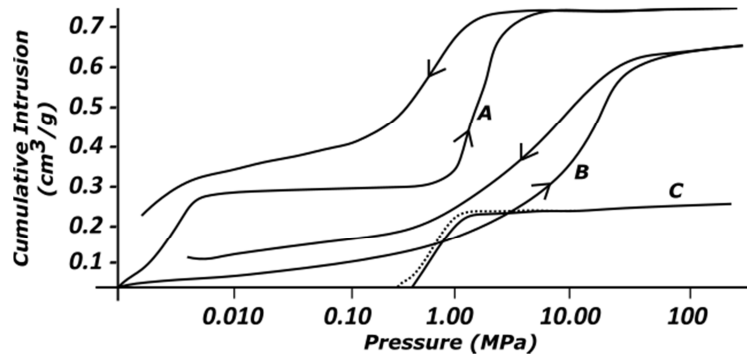


Fig. 5 Pressure-volume curves of different materials

Figure 5 shows the mercury intrusion-extrusion curves from the pores upon pressure reduction for 3 different materials: (A) sample consisting of relatively coarse grains; (B) a single piece of material in which there is a wide distribution of pore sizes (no void volume is indicated); (C) fine powder ( $\bar{\phi}=10\mu\text{m}$ ) essentially without pores and the volume is indicated due to voids among the particles. Cumulative pore volume vs. pore diameter and incremental pore volumes are the others information obtainable from application of this technique.

Micromeritics AutoPore IV 9510 (Micromeritics, Norcross, GA 30093-1877, U.S.A) equipment was used for the intrusion-extrusion porosimetry, with a range resolution in terms of pore size from 7 nm to 360  $\mu\text{m}$ . The first step for the porosimetry analysis was the standardization of the size and shape of the white and brown coconuts fibres samples. For this purpose, the samples were washed with distilled water. Subsequently the samples were oven-dried at 80 °C for 24 h, and the dry weight of the sample was determined, as shown in table 2.

Tab. 2 Hg Parameters

Advancing Contact Angle (°)	141
Receding Contact Angle (°)	141
Hg Surface Tension ( $\gamma$ - dynes/cm)	484
Hg Density (g/mL)	13.55
White coconut fibre Sample Weight (g)	0.2104
Brown coconut fibre Sample Weight (g)	0.1889

Porosimetry with mercury intrusion involves two basic steps: filling and low pressure porosimetry; the high-pressure porosimetry. The first step involves removing air and residual moisture or other liquids from the pore system. This is achieved by slowly increasing the pressure. This allows mercury to penetrate into larger pores of the sample or into any void

spaces. The first data point was taken at a pressure of 3000 Pa to 4000 Pa (0.5 psia). The last data point was taken at a pressure of 7000 Pa (1.02 psia). For the high-pressure porosimetry, the sample-cell was transferred to the high-pressure system. It was surrounded by hydraulic fluid. Pressures of up to 414 MPa (60,000 psia) were applied in an isostatic way. The intruded mercury volume was measured continuously. Table 3 shows the low pressure porosimetry parameters.

**Tab. 3** Porosimetry Parameters for Low-pressure Test

Evacuation Pressure ( $\mu\text{m}\cdot\text{Hg}$ )	50
Evacuation Time (min)	15
Mercury Filling Pressure (psia)	1.02
Equilibration Rate ( $\mu\text{L}/\text{g}/\text{s}$ )	0.1
Maximum Intrusion Volume ( $\text{mL}/\text{g}$ )	0.015

Tab. 4 shows the high pressure porosimetry parameters

**Tab. 4** Porosimetry Parameters for High-pressure Test

Equilibration Rate ( $\mu\text{L}/\text{g}/\text{s}\cdot\text{Hg}$ )	0.1
Maximum Intrusion Volume ( $\text{mL}/\text{g}$ )	0.2

## 2.2. Resin

A two-component epoxy resin with a low viscosity suitable for laminating technologies including a vacuum infusion was used as the matrix. The resin was hardened by cycloaliphatic polyamine, the main component Izoforon di-amin. The properties of the resin and the hardener according to the producer are stated in Tab. 5.

**Tab. 5** Properties of resin/hardener – technical sheet according to producer

Resin property	Resin	Hardener
Epoxy mass equivalent ( $\text{g}\cdot\text{mol}^{-1}$ )	180-196	-
Epoxy index (mol/1000g)	0.51-0.56	-
Flash-point	>150	-
Viscosity mPa.s at 25°C	500-900	7-11
Density ( $\text{g}\cdot\text{cm}^{-3}$ )	1.12-1.16	930-960
Hydrogen equivalent (g)	-	48

## 2.3. Composite

The preparation of composite boards (see Fig. 6) was performed by means of the vacuum infusion. Settled fibres which were pressed by the force 5 kN were put into the prepared moulds in a shape of the board with dimensions 20 x 30 cm and a height of 4 mm.

The composite was prepared with 20 wt. % of the fibres in the epoxy matrix. The space of the mould was treated at first by a liquid separator which is of zero adhesion to the resin. The mould space was closed by means of the vacuum mass/tape and then filled with the resin. A vacuum pump with the following parameters: capacity  $55 \text{ l}\cdot\text{min}^{-1}$  and the absolute pressure of 100 mbar abs was used for the vacuum process.

The test samples were cut from the boards by means of an abrasive water jet, see Fig. 6.



**Fig. 6** Process of composite board preparation and cutting test samples by water jet

The hardness was evaluated at the prepared composite boards, namely by means of a ball indenter of the diameter 5 mm and the force 961 N according to the standard CSN EN ISO 2039. The test samples for the tensile strength corresponded to the standard CSN EN ISO 3167. Samples were tested on a universal testing machine. A speed of a cross beam motion was  $6 \text{ mm}\cdot\text{min}^{-1}$ . The setting for tensile characteristics test was performed in accordance with the standard CSN EN ISO 527.

### 2.3.1. Wear resistance testing

A three-body abrasion resistance was evaluated on a device defined in the standard 23.208-79 [23] (Wear resistance testing of materials by friction against loosely fixed abrasive particles, see Fig. 7). Free abrasive particles of sand of a size  $100 - 200 \mu\text{m}$  were strewn on a

test sample of a dimension 30 x 30 x 4 mm to which rubber disc of a diameter 50 mm and a width 15 mm was pressed at the same time. 1000 turns were realized which corresponds to the rubber disc track of a length 157 m. A peripheral speed of the rubber disc corresponded to  $0.162 \text{ m}\cdot\text{s}^{-1}$ . The rubber disc was pressed to the test sample surface by 1.58 kg. Test samples were weighed always before and after the test with a sensitivity to 0.1 mg. Mass losses were recorded.

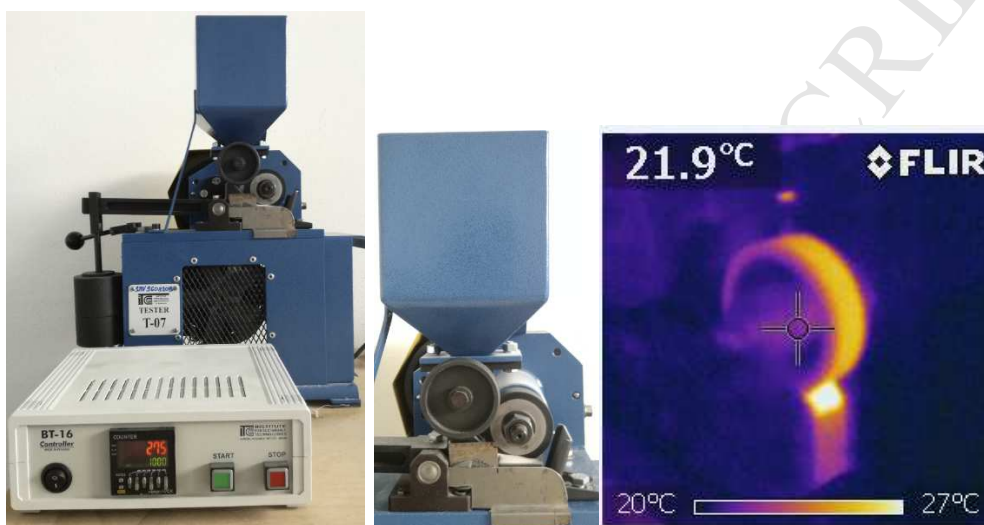


**Fig. 7** From left: Test equipment, detail of rubber disc, temperature of rubber disc during test (after 750 turns)

The interfacial interaction, the fracture surfaces, the morphology and the microstructure of coir fibres were evaluated by means of the electron microscopy – Tescan Mira 3 GXM. The samples were dusted with gold for the purpose of the electron microscopy.

ANOVA analysis and T-test in the significance level  $\alpha = 0.05$  were used for the statistical evaluation of the experimentally gained data. Introduced zero hypothesis  $H_0$  speaks about the statistically insignificant difference in the observed characteristics among compared sets of data, i.e.  $p > 0.05$ .

### 3. Results and discussion

Dimensions of the fibres were determined by means of the stereoscopic and electron microscopy. The diameter of the brown coir ( $243 \pm 68 \mu\text{m}$ ) was of  $31 \mu\text{m}$  higher on average

than the diameter of the white coir ( $212 \pm 56 \mu\text{m}$ ). The measurement results are summed up in the histogram – Fig. 8.

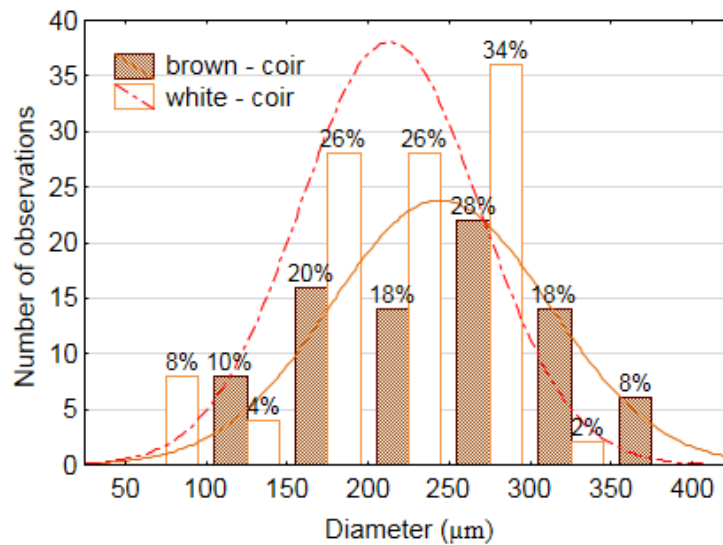


**Fig. 8** Histogram: diameter of brown and white coir fibres

There is no difference between the brown and the white coir in the fibre structure. The fibres are created from single elementary fibres which are hollow. A lacuna is visible in the middle, see Fig. 9. The structure detail is obvious from Fig. 10.

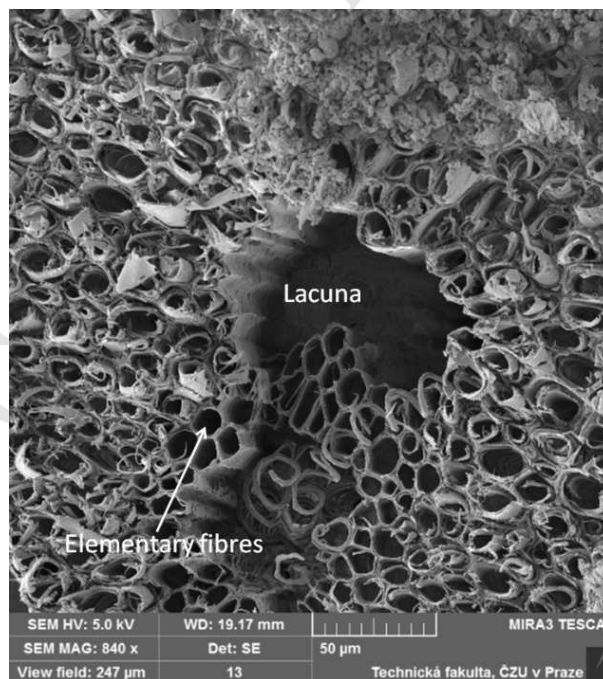


**Fig. 9** SEM images of cross section (white coir) Mag. 840 x

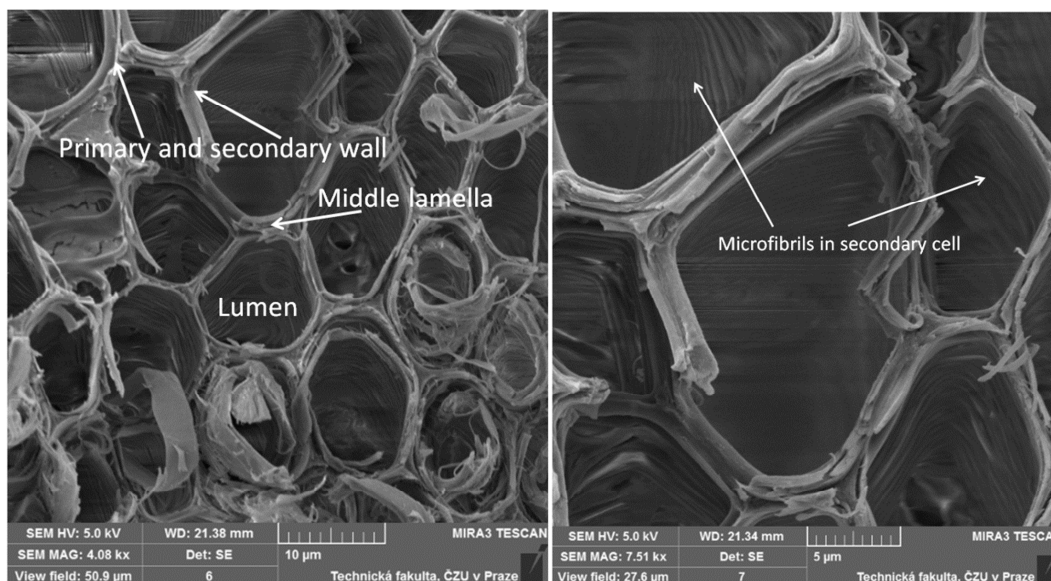


**Fig. 10** Detail of elementary fibres (brown coir): Mag. 4.08 kx (left), Mag. 7.51 kx (right)

Table 6 shows the results of the mercury porosimetry for the white and brown coconut fibres. The volume of the pore was 0.6578 mL/mg for the white coconut fibres that corresponded to a maximum mercury pressure of 59936.04 (psia) as shown in Fig. 11a. And of 0.7645 mL/mg for the brown coconut fibres that corresponded to a maximum mercury pressure of 59933.02 (psia) as shown in Fig. 11b. The pore diameter value was approximately 3.6 nm for mercury pressure values of 59936.04 (psia) for the white coconut fibres, and for mercury pressure values of 59933.02 (psia) for the brown coconut fibres. The maximum pore diameter value was approximately 214.1 and 217.1(µm), for white and brown coconut fibres respectively, for a low-pressure of 1.02 (psia).

**Tab.6** Results of Porosimetry

	White Coconut <b>Fibres</b>	Brown Coconut <b>Fibres</b>
Total Intrusion Volume	0.6578 mL/g	0.7645 mL/g
Total Pore Area	22.618 m <sup>2</sup> /g	14.373 m <sup>2</sup> /g
Median Pore Diameter (Volume)	555.4 µm	751 µm
Median Pore Diameter (Area)	13.8 nm	6.6 nm
Average Pore Diameter (4V/A)	0,1163 µm	0.2128 µm
Bulk Density at 1.02 psia	0.709 g/mL	0.664 g/mL
Apparent (Skeletal) Density	1.3284 g/mL	1.3486 g/mL
Porosity	46.64 %	50.77 %
Stem Volume Used	36 %	38 %

The results of the porosimetry of the fibres show that the maturation process of the fibres increases the porosity. In fact, the porosity for the white coconut fibres is 46.64 %, and for the brown coconut fibres is 50.77 %.

while, for the brown coconut fibres the porosity is 50.77 % (tab. 6). It is possible to note from the same table that the average pore diameter of the cylinder-shaped pores was of 0.1163  $\mu\text{m}$  and of 0.2128  $\mu\text{m}$ , for the white and brown coconut fibres respectively.

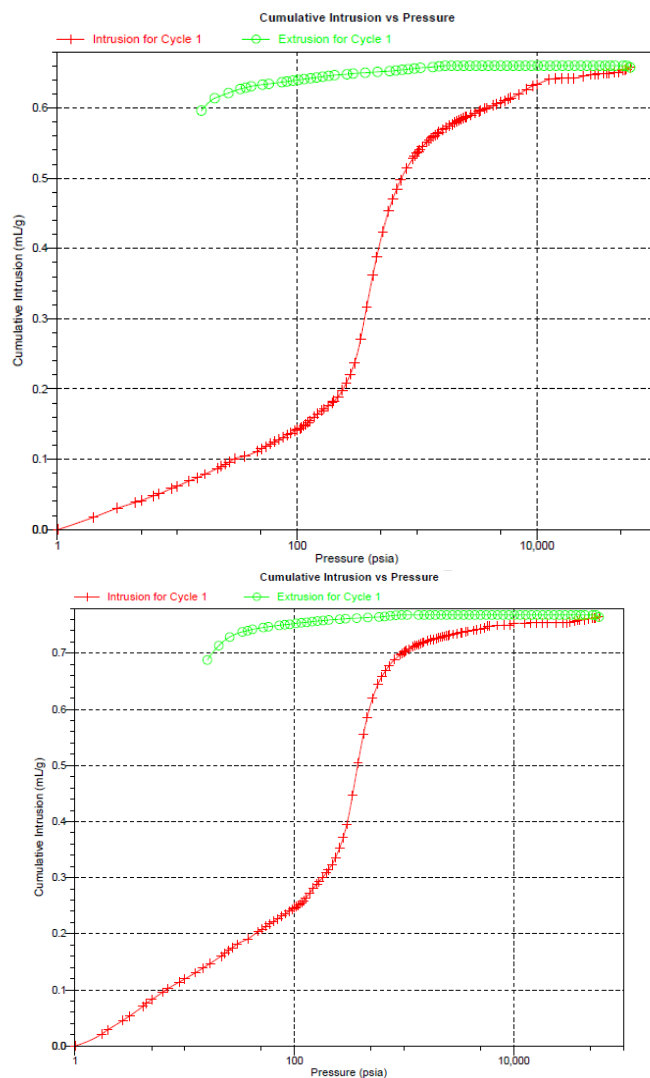


**Fig. 11** Cumulative intrusion vs pressure for: a) white coir (above); b) brown coir (bottom)

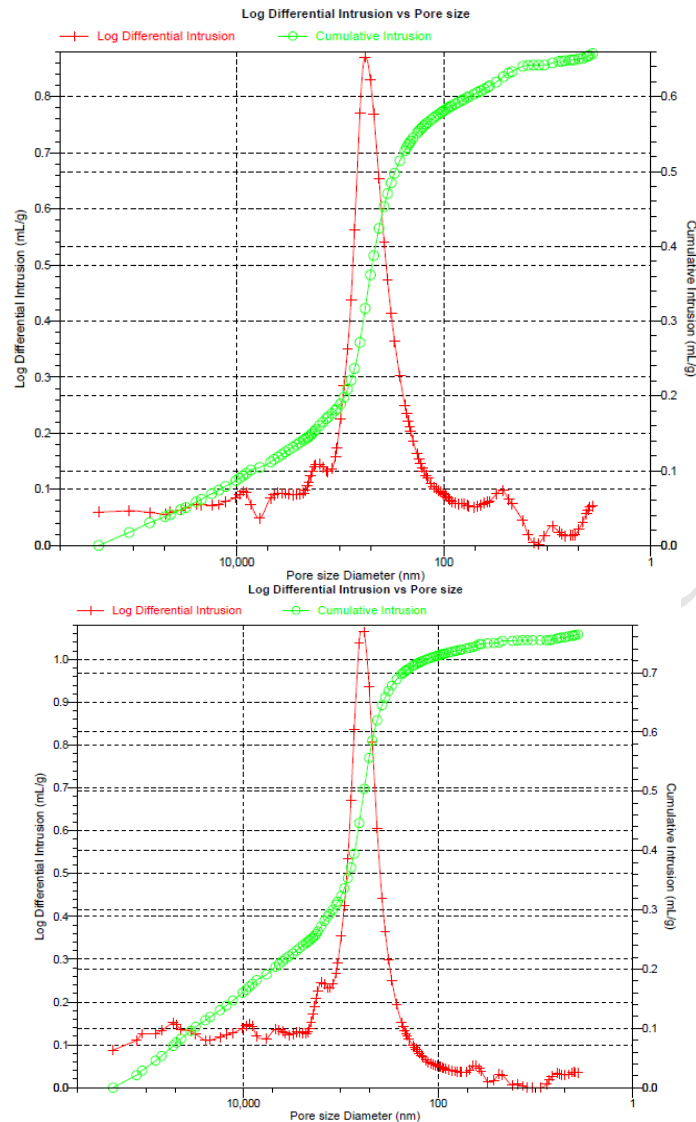


**Fig. 12** Log differential intrusion vs pore size for: a) white coir (above); b) brown coir (bottom)

The figures 12a and 12b show the hysteresis curves for white and brown coconut fibres, respectively. From these figures it has been possible to investigate on the pore shape of the fibres under study. In fact, from the comparison of the results presented by Liabastre and Orr [30] and Zgrablich et al. [31] it is possible to conclude that the intrusion and extrusion curves at the highest test pressure have the same pattern of the hysteresis curves of the needles pore shape and spherical pore shape [30, 31]. The influence of the surface treatment by 6 % water solution of NaOH on the surface of the fibres is illustrated in Fig. 13. The alkali acting increased the surface texture of the fibres which is clearly observable. This process is caused due to removing of natural and artificial impurities from the fibre surface, i.e. e.g. the



cellulose amount. The arrangement of units in the cellulose macromolecule changed at the same time [32]. Spherical formations – globular particles are visible on the surface before the alkali treatments of the coir fibres. These formations are removed from the surface owing to the chemical treatment. The lignin layers – phenolic natural polymer are marked in Fig. 14 (left). The significant removal of these layers occurs due to the alkali treatment. The surface shape optimization due to the described changes leads to an improvement of the interfacial interaction with used matrices. Nam et al. [16] summarize the influence of the alkali acting on the coir surface by the schema [33] (5):

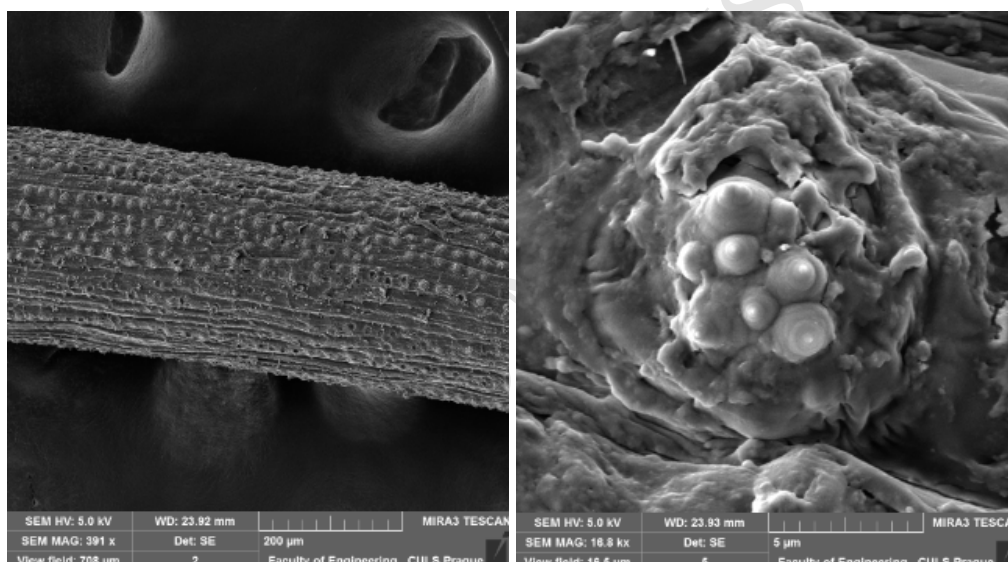
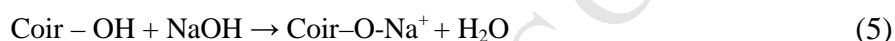


**Fig. 13** Brown coir – microstructure of brown coir before chemical treatment - Mag. 391 x (left), detail of globular surface formations (Silica body) – Mag. 16.8 kx (right)

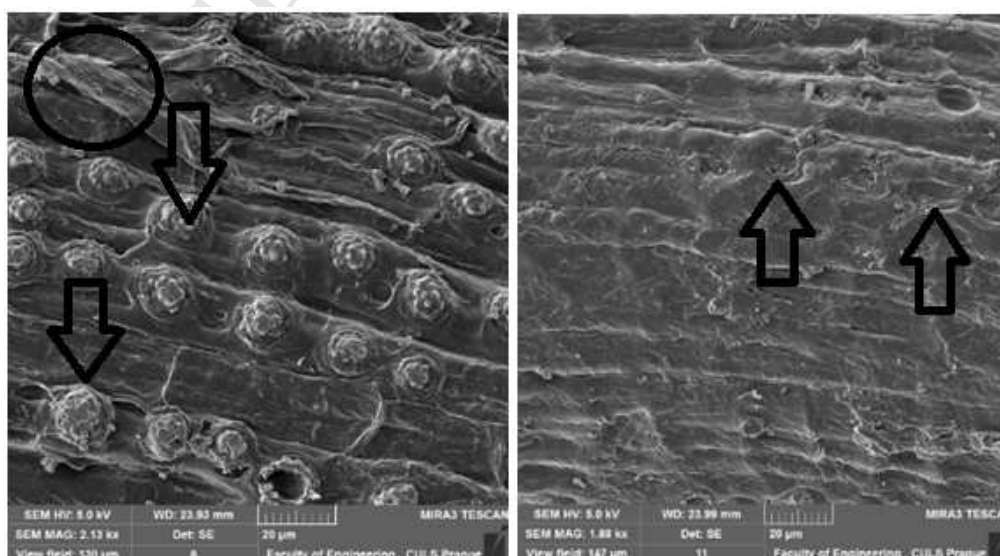


**Fig. 14** Brown coir – fibre surface before chemical treatment by alkali - Mag. 2.13 kx (left), fibre surface after chemical treatment Mag. 1.88 kx (right)

The lignin works at the cuticulas as the adhesive in the cell walls of cellulose fibres. It indicates their structure and protects the fibres against microbial or chemical degradation. The observation of the influence of the alkali treatment on the fibre surface is in accordance with conclusions of authors [34-36]. A disappearance of surface globular formations would become more intensive, according to their conclusions, due to increased expiration length, e.g. 72 h.

Further the influence of the chemical treatment on the strength characteristics of fibres was judged, namely by means of the tensile strength and the modulus of elasticity, see Fig. 15. The tensile strength of the brown untreated fibre reached the value  $123 \pm 54$  MPa (2.53 GPa) on average and the alkali treatment increased this value of 58 MPa (of 1.87 GPa). The value of the tensile strength at the white fibres reached  $115 \pm 33$  MPa ( $2.40 \pm 059$  GPa) and the alkali treatment increased this value of 36 MPa (0.49 GPa).

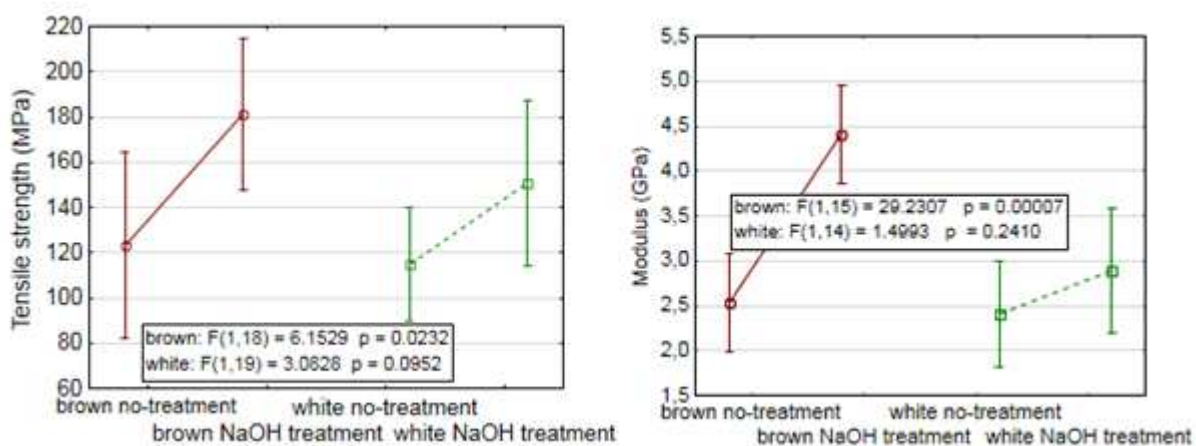


**Fig. 15** Strength characteristics of fibres before and after alkali treatment: tensile strength (left), modulus of elasticity (right)

Results described in the experiment are in accordance with the results of other studies – however, most authors state the strength of the coir fibres without a definition of their harvest stadium – i.e. the properties of the brown fibres in a full maturation of the coconut. Yan et al. [13, 14] state the tensile strength of the coir 95 – 230 MPa, the elastic modulus 2.8

– 6.0 GPa. Nele Defoirdt et al. [11] differed various stadiums of the maturation and they determined the tensile strength of the white coir as  $162 \pm 32$  to  $192 \pm 37$  MPa and of the brown coir as  $186 \pm 55$  to  $343 \pm 36$  MPa. They determined the elastic modulus as 3.39 GPa at the white coir fibres and as 4.16 GPa at the brown coir fibres. Generally, the interval 4 – 6 GPa is presented in the literature [37, 38]. Ramakrishna and Sundararajan [39] state the interval 15 – 327 MPa and Toledo et al. [40] 108 - 252 MPa. Generally, it is possible to say that the experimentally ascertained tensile strength values of the fibres at single available studies very differ [15].

The statistical comparison of the fibre tensile strength (T-test) in the significance level  $\alpha = 0.05$  talks about the statistically significant increase of the tensile strength of the brown fibres after the alkali treatment ( $p = 0.02$ ). This increase was not statistically significant in this level at the white fibres ( $p = 0.42$ ), namely due to a high dispersion which can be caused by the natural character of judged fibres.

The alkali treatment of the fibre surface led identically with the results of the authors [16, 33] to the increase of the tensile characteristics of the fibres. Nam et al. [16] describe the strength increase due to the acting of NaOH from 139.67 MPa to the value 218.52 MPa (5% solution of NaOH, acting time 24 h). The modulus was increased by this treatment from 2.79 GPa to 5.64 GPa. However, it is possible to find in the literature also results which describe the fall of the tensile characteristics due to the alkali treatment, e.g. the study of Imran and Adelbert [35]. They justify the results by a fall of binding elements in the fibres. However, the tensile strength increase due to the suitable alkali treatment is described also in many other studies [17, 35].

The chemical treatment of the fibres led to the optimization of the interfacial interaction which was observable by means of the electron microscopy. This fact was caused by a removal of the surface layers and the globular formations manifesting itself by the fibre

surface roughening which was reflected in better wetting of the fibres with the matrix. Higher roughness of the fibre surface without undesirable formations also increases the mechanical interfacial bond. The rise of the imperfect wetting – gaps – between the matrix and the fibre is visible in Fig. 16 (left). The example of the optimum wetting is presented in Fig. 16 (right).

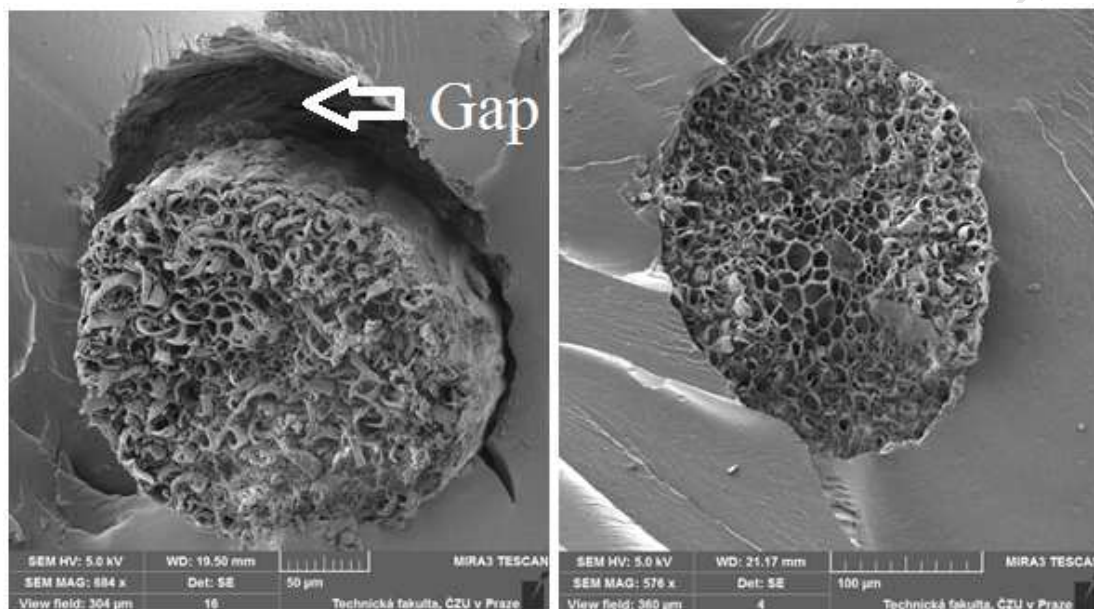


**Fig. 16** Fracture surface – detail of interfacial interaction: bad interaction (left), optimum interaction (right)

Assumptions gained by the electron microscopy were subsequently certified by the experimental program describing the strength characteristics of the composite systems with long oriented coconut white and brown fibres. The concentration 20 wt. % was used for the description of the difference between the composite strength of white or brown fibres – namely according to the conclusions of Nam et al. [16] who describe a significant increase of the strength from 5 to 25 wt. % of the coir fibres. However, the composite with 30 wt. % of the fibres was already of smaller strength than the composite with 25 wt. % of the fibres (the matrix: butylene succinate). So the concentration 20 wt. % was chosen as the optimum concentration for the comparison of the properties of the composite with the white and the brown fibres.

The tensile strength of the epoxy resin was increased due to the inclusion of the coir. This increase was caused by higher tensile strength and modulus of the fibres in a comparison

with the epoxy matrix. The increase of the composite strength occurred by the inclusion of the brown fibres, of 25.54 MPa at the untreated fibres and of 28.64 MPa at the treated fibres. The strength was increased of 19.69 MPa (untreated fibres), resp. of 20.22 MPa (NaOH treatment) at the composite with the white fibres. These materials are mostly loaded with higher dispersion of measured values owing to the natural character of described composite systems. This dispersion causes the fact that if the values between the treated and untreated fibres (T-test) in the significance level  $\alpha = 0.05$  are compared, the parameter  $p$  is  $p > 0.05$  for the brown fibres and for the white fibres.

Results correspond with the conclusions of many authors [31, 39-42] as well as of Nam et al. [16], who observed the increase of the matrix strength of 28.2 % at the same concentration due to the inclusion of the brown untreated fibres and of 71.8 % at fibres treated with NaOH for 72 h. The increase of the elongation at break, Fig 17 right, is in accordance with the conclusion of Huang Gu [43] who observed the increase of the elongation at break at PP/coir composite with the fibres treated with 10 % NaOH from the value 14.5 % to the value 18.9 %.

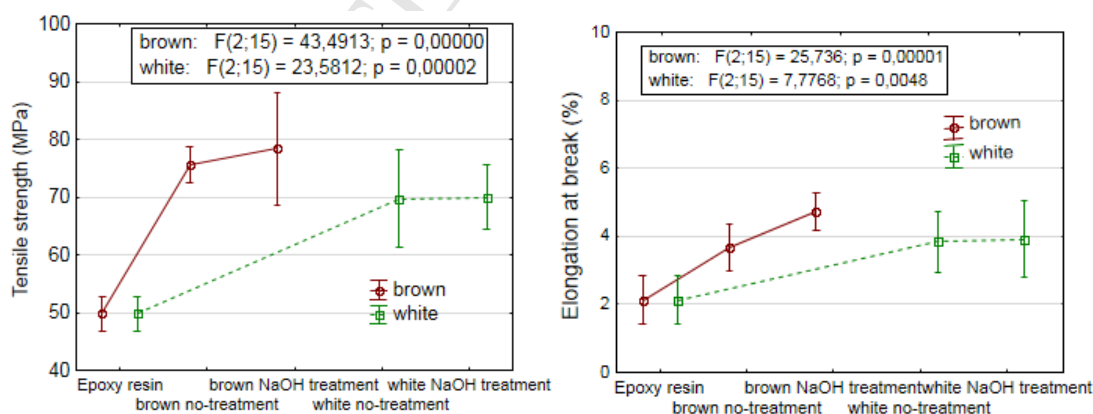


**Fig. 17** Strength characteristics of composite systems: tensile strength (left), elongation at break (right)

The hardness of the prepared composites was declining in a comparison with the unfilled resin, see Fig. 18. There is no statistically significant difference between the hardness of the composites with treated as well as untreated fibres and with brown and white fibres: always  $p > 0.05$ .

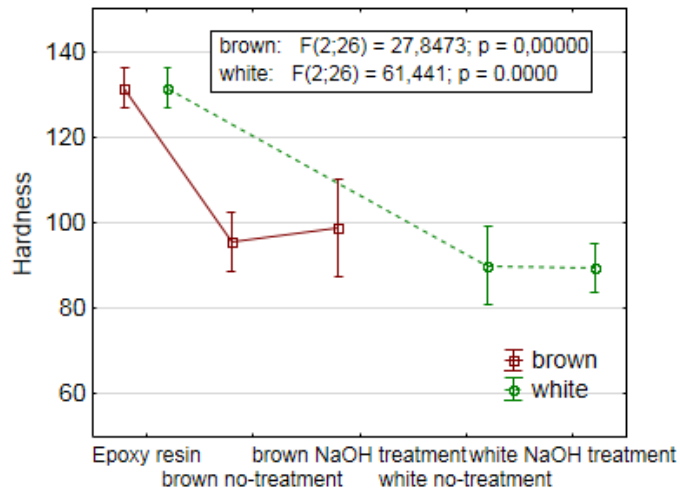
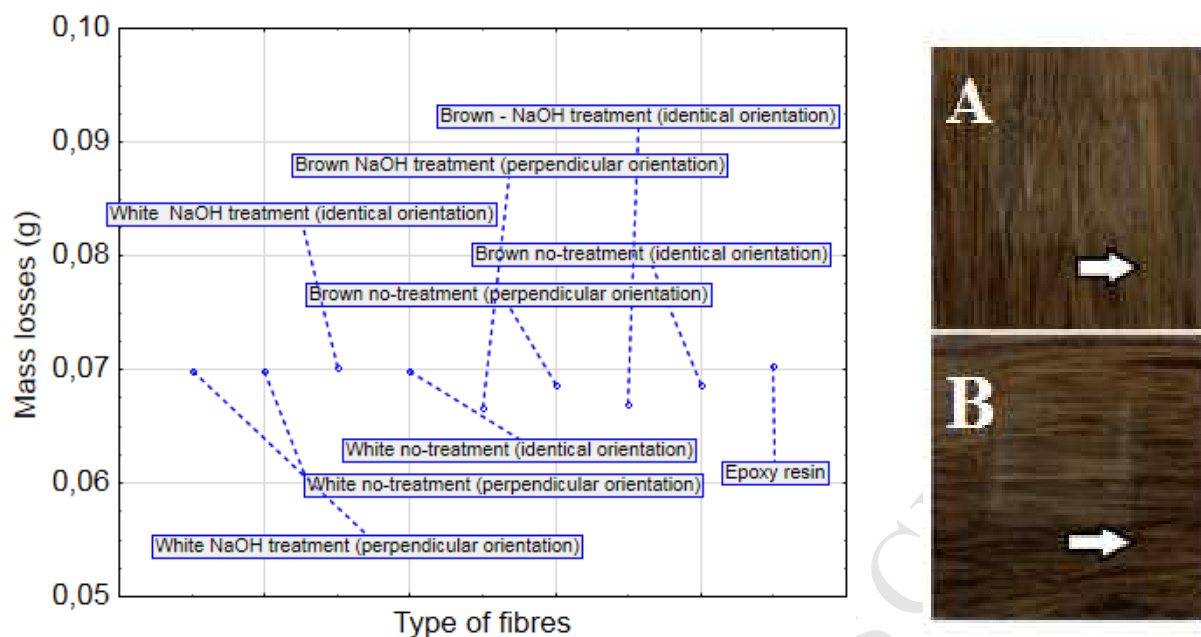


Fig. 18 Hardness of composite systems - CSN EN ISO 2039

Results of the abrasive wear resistance are presented in Fig. 19. It is obvious from the results that fibres were of no high influence on resultant losses. Significant differences between white and brown coir fibres were not proved. Differences between the fibres orientation – oriented in a direction of the rubber disc rotation and perpendicular to the direction of the rubber disc rotation - were not recorded at the same time. The loss of the resin without the filler corresponded to 0.0703 g. The highest increase in wear resistance (0.0666 g) was recorded at the body with perpendicular fibres orientation to the direction of the rubber disc (brown coir, NaOH treatment) – it was an increase of 5 %. The perpendicular orientation of the fibres to the direction of the rubber disc slightly increased resistance to wear. The NaOH treatment did not have an impact on wear resistance. These results are in agreement with those of [44]. In fact, a better result on wear resistance depends not only on the hardness of the individual components that make up the composite material, but also on its porosity [44] and its Median Pore Diameter (Area) (Tab. 6). In fact, for the porous materials, with high Median Pore Diameter (Area), abrasive grains can enter the pores dropping drastically the wear-resistance. In the cases under study, the best wear resistance is obtained in the case of composites with brown coconut fibres, which corresponds to a greater porosity, to a greater hardness and to a lower value of Median Pore Diameter (Area) (Tab. 6).



**Fig. 19** Resistance to abrasive wear (left), arrow (right) indicates direction of disc rotation: A-perpendicular orientation; B-identical orientation

#### 4. Conclusions

The structure of fibres described by the electron microscopy certified the presence of fibre cavities – pores. The structure and the morphology of the brown and the white fibres are very similar. The coir fibres are of high ductility at the low relative mass. The suitable alkali treatment increases their tensile strength and the elastic modulus. Used alkali treatment 6 % water solution of NaOH for 12 h removed a huge amount of undesirable surface formations/layers on the fibres. It was certified by SEM analysis. This treatment led to the increase of the tensile strength of both brown as well as white fibres. The tensile strength of the composite systems was increased due to the performed alkali treatment which was a consequence of the optimization of the interfacial interaction. The optimization of the interaction was observable by the electron microscopy when it came to better wetting of the fibres with the epoxy matrix.

The primary aim of the experiment was not to judge the influence rate of various alkali treatments on the tensile characteristics of the fibres and the composites. However, it is

obvious that longer time of the alkali treatment would lead to the improvement of the observed characteristics.

It is possible to say by comparing the characteristics of the brown and the white fibres and the composite systems created with these fibres that the brown fibres reach higher tensile strength than the white fibres. The composite systems created with brown fibres reach also better mechanical characteristics. Important conclusions from the performed experiment can be summarized in a following way:

- The results of the porosimetry show that brown coconut fibres have a higher porosimetry ratio than white coconut fibres.
- In addition, brown coconut fibres have an average pore diameter value, using the cylinder-shaped pores approximation, of about 82% higher than pores of white coconut fibres. This finding is an important factor at forming mechanical characteristics of fibres and their composite systems.
- The hardness was decreased up of 32 % due to the inclusion of the fibres.
- The alkali treatment at the brown fibres increased the tensile strength of 47 % and the modulus of 74 %
- The alkali treatment at the white fibres increased the tensile strength of 31 % and the modulus of 20 %.
- The composites with the brown fibres reached higher tensile strength than the composites with the white fibres. This fact can be influenced by a difference of the fibre porosity which was proved by this study when the pores can be filled with the resin in some situations.
- The alkali treatment of the fibres increased the tensile strength at the composite systems with the brown fibres of 3.7 %. This increase was negligible 0.4 % at the white fibres.



- The best wear resistance is obtained in the case of composites with brown coconut fibres, which corresponds to a greater porosity, to a greater hardness and to a lower value of Median Pore Diameter (Area).

#### **ACKNOWLEDGMENTS**

This paper was made with the assistance of the grant IGA TF CZU 2017:31140/1312/3113 and the Italian FARB 2016. The research was conducted thanks to the cooperation between the Department of Material Science and Manufacturing Technology of the Czech University of Life Sciences Prague (CULS), Faculty of Engineering, Applied Mechanics Lab of the Department of Industrial Engineering of the University of Salerno (IT), and the University Politecnica de Madrid, Spain.

## References

- [1] Lau K, Hung P, Zhu MH, Hui D. Properties of natural fibre composites for structural engineering applications: *Composites Part B: Engineering* 2018;136:222–233.
- [2] Elsabbagh A, Steuernagel L, Ring J. Natural Fibre/PA6 composites with flame retardance properties: Extrusion and characterization: *Composites Part B: Engineering* 2017;108(1):325–333.
- [3] Ruggiero A, Valášek P, Müller M. Exploitation of waste date seeds of *Phoenix dactylifera* in form of polymeric particle biocomposite: Investigation on adhesion, cohesion and wear: *Composites Part B: Eng* 2016;104(1):9–16.
- [4] Guilherme Piovezan O, Murilo Pereira M, Gizilene C, Andrelson WR, Silvia LF. Mechanical properties of a polyurethane hybrid composite with natural lignocellulosic fibers: *Composites Part B: Engineering* 2017;110(1):459–465.
- [5] Feo L, Latour M, Penna R, Rizzano G. Pilot study on the experimental behavior of GFRP-steel slip-critical connections: *Composites Part B: Engineering* 2017;115:209–222.
- [6] Fascetti A, Feo L, Nisticò N, Penna R. Web-flange behavior of pultruded GFRP I-beams: A lattice model for the interpretation of experimental results: *Composites Part B: Engineering* 2016;100:257–269.
- [7] Barretta R, Feo L, Luciano R, Marotti de Sciarra F, Penna R. Functionally graded Timoshenko nanobeams: A novel nonlocal gradient formulation: *Composites Part B: Engineering* 2016;100:208–219.
- [8] Feo L, Fraternali F, Skelton RE. Special issue on composite lattices and multiscale innovative materials and structures: *Composites Part B: Engineering* 2017;115:1–2.
- [9] Madyan OA, Fan M, Feo L, Hui D. Enhancing mechanical properties of clay aerogel composites: An overview: *Composites Part B: Engineering* 2016;98:314–329.
- [10] Fowler PA, Hughes JM, Elias RM. Biocomposites: Technology, environmental credentials and market forces: *Journal of the Science of Food and Agriculture* 2006; 86(12):1781–1789.
- [11] Defoirdt N, Biswas S, et al. Assessment of the tensile properties of coir, bamboo and jute fibre: *Composites Part A: Applied Science and Manufacturing* 2010;41(5):588–595.
- [12] Geethamma VG, Mathew KT, Lakshminarayanan R, Thomas S. Composite of short coir fibres and natural rubber: effect of chemical modification, loading and orientation of fibre. *Polymer* 1998;39(6–7):1483–91.
- [13] Yan L, Kasal B, Huang L. A review of recent research on the use of cellulosic fibres, their fibre fabric reinforced cementitious, geo-polymer and polymer composites in civil engineering: *Composites Part B: Engineering* 2016;92:94–132.
- [14] Yan L, Chouw N, Jayaraman K. Flax fibre and its composites – a review: *Composites Part B* 2014;56:296–317.
- [15] Ali M. Coconut fibre: A versatile material and its applications in engineering: *Journal of Civil Engineering and Construction Technology* 2011;2(9):189–197.
- [16] Nam TH, Ogihara S, Tung TH, Kobayashi S. Effect of alkali treatment on interfacial and mechanical properties of coir fiber reinforced poly(butylene succinate) biodegradable composites: *Composites Part B: Engineering* 2011;42(6):1648–1656.

- [17] Komuraiah, NS, Kumar, BD, Prasad. Chemical composition of natural fibres and its influence on their mechanical properties: *Mech Compos Mater* 2014;50(3):359–376.
- [18] Easwara Prasad GL, Keerthi Gowda BS, Velmurugan RA. Study on Impact Strength Characteristics of Coir Polyester Composites: *Procedia Engineering* 2017;173:771–777.
- [19] Jia Yao, Yingchang Hu, Wen Lu. Performance Research On Coir Fiber And Wood Debris Hybrid Boards: *BioRes* 2012;7(3):4262–4272.
- [20] Jawaid M, Abdul Khalil HPS. Cellulosic/synthetic fibre reinforced polymer hybrid composites: a review. *Carbohydr Polym* 2011;86(1):1–18.
- [21] Jie Wei, Yubao Li, Kin-Tak Lau, Preparation and characterization of a nano apatite/polyamide6 bioactive composite, *Composites Part B: Engineering* 2007;38(3); 301-305.
- [22] Jiandong Zhuang, Seyed Hamidreza Ghaffar, Mizi Fan, Jorge Corker, Restructure of expanded cork with fumed silica as novel core materials for vacuum insulation panels, *Composites Part B: Engineering* 2017; 127:215-221.
- [23] GOST 23.208-79. A Method for Tests of Materials for Wear Resistance in Friction against Nonrigidly Fastened Abrasive Particles [in Russian], Izd. Standartov, Moscow (1984).
- [24] Krolczyk GM, Maruda RW, Nieslony P, Wieczorowski M. Surface morphology analysis of Duplex Stainless Steel (DSS) in Clean Production using the Power Spectral Density: Measurement: *Journal of the International Measurement Confederation* 2016;94(1):464–470.
- [25] Sharma V, Chattopadhyaya S, Hloch S. Surface quality finish in laser cutting using Taguchi design: *Tehnicki Vjesnik* 2017;24:15–19.
- [26] Krolczyk GM, Krolczyk, JB, Maruda RW, Legutko S, Tomaszewski, M. Metrological changes in surface morphology of high-strength steels in manufacturing: Measurement: *Journal of the International Measurement Confederation* 2016;88:176–185.
- [27] Jaber, S. A., Ruggiero, A., Battaglia, S., & Affatato, S. On the roughness measurement on knee prostheses. *The International journal of artificial organs*, 2015; 38(1), 39-44. DOI: 10.5301/ijao.5000371
- [28] Washburn EW. Note on a Method of Determining the Distribution of Pore Sizes in a Porous Material: *Proc. Natl. Acad. Sci. U. S. A.* 1921;7(4):115–116.
- [29] Adamson AW. (Alice P. Gast, Physical chemistry of surfaces. Wiley, 1997.
- [30] Liabastre AA, Orr C. An evaluation of pore structure by mercury penetration: *J. Colloid Interface Sci.* 1978;64(1):1–18.
- [31] Zgrablich G, et al. Effect of porous structure on the determination of pore size distribution by mercury porosimetry and nitrogen sorption: *Langmuir* 1991;7(4):779–785.
- [32] Valadez-Gonzalez A, Cervantes-Uc, JM, Olayo, R, Herrera-Franco, PJ. . Effect of fiber surface treatment on the fiber–matrix bond strength of natural fiber reinforced composites: *Composites Part B: Engineering* 1999;30(3):309–320.
- [33] Rahman, MM, Khan, MA. Surface treatment of coir (*Cocos nucifera*) fibers and its influence on the fibers' physico-mechanical properties: *Compos Sci Technol* 2007;67:2369–2376

- [34] Hong Sheng Tan, Yuan Zhang Yu, Lin Lin Liu, Li Xue Xing. Effect of Alkali Treatment of Coir Fiber on Its Morphology and Performance of the Fiber/LLDPE Bio-Composites: *Advanced Materials Research* 2010;139-141:348–351.
- [35] Prasad SV, Pavithran C, Rohatgi PK. Alkali treatment of coir fibers for coir–polyester composites: *J Mater Sci* 1983;18:1443–1454.
- [36] Imran SM, Adelbert T. Effect of Alkali Treatments of Physical and Mechanical Properties of Coir Fiber: *Chemical and Materials Engineering* 2015;3(2):23–28
- [37] Bledzki AK, Gassan J. Composites reinforced with cellulose based fibres: *Prog Polym Sci* 1999;24(2):221–274.
- [38] Silva GG, De Souza DA, Machado JC, Hourston DJ. Mechanical and thermal characterization of native Brazilian coir fiber. *J Appl Polym Sci* 2000;76(7):1197–206.
- [39] Ramakrishna G, Sundararajan T. Studies on the durability of natural fibres and the effect of corroded fibres on the strength of mortar: *Cement and Concrete Composites* 2005;27(5):575–582.
- [40] Toledo Filho R D, Ghavami K, England GL. Free, restrained and drying shrinkage of cement mortar composites reinforced with vegetable fibres: *Cement and Concrete Composites* 2005;27(5):537–546.
- [41] Rout J, Tripathy SS, Misra M, Mohanty AK, Nayak SK. The influence of fiber surface modification on the mechanical properties of coir–polyester composites: *J Appl Polym Sci* 2001; 22:468–476.
- [42] Fairuz I. Romli, Ahmad Nizam Alias, Azmin Shakrine Mohd Rafie, Dayang Laila Abang Abdul Majid. Factorial Study on the Tensile Strength of a Coir Fiber Reinforced Epoxy Composite: 2012 AASRI Conference on Modelling, Identification and Control AASRI Procedia 3 2012;242–247.
- [43] Huang Gu. Tensile behaviours of the coir fibre and related composites after NaOH treatment: *Materials & Design* 2009;30(9):3931–3934.
- [44] Khruschov, M. M. "Principles of abrasive wear." *wear* 1974;28(1):69-88.